EFFECT OF WALL BOUNDARY CONDITIONS ON 3D HYDRODYNAMIC NUMERICAL SIMULATION OF A CLC UNIT WITH DUAL CIRCULATING FLUIDIZED-BED REACTORS

Liyan Sun[1], Enrica Masi[1*], Olivier Simonin[1],

Øyvind Langørgen[2], Inge Saanum[2], Nils Erland L. Haugen[2]

[1]*Institut de Mécanique des Fluides de Toulouse* (*IMFT*)*, Université de Toulouse, CNRS, Toulouse, France*

[2]*Department of Thermal Energy, SINTEF Energy Research, Trondheim, Norway*

*Email: *enrica.masi@imft.fr*

Abstract

3D unsteady numerical simulations of a chemical looping combustion (CLC) unit constructed at SINTEF Energy Research (Trondheim, Norway) are performed with the goal to investigate the effect of the particle-wall boundary conditions on the CLC flow behavior. Simulations are carried out using NEPTUNE_CFD, a simulation tool based on a two-fluid modelling approach. Three types of boundary conditions are used for the solid phase: free-slip, no-slip and friction conditions. Comparison between predictions shows that the dominant frictional effect on the particle phase velocity is due to the long-time frictional contact of the particles with the wall. Results show that different boundary conditions may have an effect on the pressure distribution because of the modification of the flow behavior inside the reactors. Noteworthy is the effect that such a modification entails on the different parts of the system because of their coupling.

Introduction

Chemical looping combustion (CLC) allows to control CO_2 emissions by CO_2 separation from the combustion products with a very low energy penalty (Lyngfelt et al. 2011). It is now a well-established technology, intended for use on an industrial scale. New processes based on this technology are being developed and they need as much information as possible to design units that ensure efficiency along with low costs. In this regard, the three-dimensional (3D) numerical simulations may help in both the development and scale-up stages, especially when understanding the instantaneous and local behavior of the flow is crucial for optimizing some parts of the CLC system. In present work, a multiphase computational-fluid-dynamics (CFD) strategy is used to investigate the flow behavior of an existing CLC pilot constructed at SINTEF Energy Research (Trondheim, Norway). Such a strategy uses a two-fluid model approach which is well known to allow numerical simulations at larger scales. This approach relies on the modeling of the particulate flows inside the flow as well as at the wall. The present study aims at investigating the effect of the particle-wall boundary conditions (BC) on the CLC predictions. Three different BC are tested: free-slip, no-slip and friction conditions, with a given set of particle/wall interaction parameters. Results are mainly analyzed on the basis of the time-averaged relative pressure predictions comparing with experimental measurements.

Mathematical models

The two-fluid model implemented in NEPTUNE_CFD has been used to predict the local and instantaneous behavior of both the gas and solid phases under isothermal conditions. Details about the whole modeling may be found in previous works (see, for example, Hamidouche et al. 2019). The present study is focusing on the effect of particle-wall BC on the hydrodynamic of the dual circulating fluidized bed reactor systems. The wall BC for the particle phase consist in the modelling of the mean particle tangential momentum and random kinetic energy fluxes

at the wall, namely at a particle center distance $d_p/2$, where d_p is the particle diameter. Particle-wall BC may be written in the very general form as

$$\left(\mu_p \frac{\partial U_{p,\tau}}{\partial n}\right)_{wall} = \Sigma_{w,\tau n} \quad (1)$$

$$\left(\lambda_p \frac{\partial q_p^2}{\partial n}\right)_{wall} = \phi_w \quad (2)$$

where $\Sigma_{w,\tau n}$ and ϕ_w represent, respectively, the mean particle tangential momentum and random kinetic energy fluxes transferred by the particle assembly to the wall. The unit vector normal to the wall, $\mathbf{n}$, is directed towards the flow, and the unit vector tangent to the wall, $\boldsymbol{\tau}$, is given as colinear to the projection of the particle velocity on the wall. Accordingly, the tangential particle velocity component is written as $\mathrm{U_{p,\tau}}=\left|\mathbf{U_p}-\left(\mathbf{U_p}.\mathbf{n}\right)\mathbf{n}\right|$. In Eqs. (1) and (2), μ_p and λ_p are the particle dynamic viscosity and random kinetic energy diffusivity which account for the transport within the particle assembly due to kinetic, collisional and frictional effects.

$\Sigma_{w,\tau n}$ and ϕ_w depend on how the discrete particles interact with the wall and, in particular, may be a function of the elastic normal and tangential restitution coefficients, of the friction coefficient, as well as of the wall roughness. In the simplest case, the BC may be derived by assuming pure elastic frictionless bouncing of the particles on a flat wall and are written as

$$\left(\mu_p \frac{\partial U_{p,\tau}}{\partial n}\right)_{wall} = 0 \quad (3)$$

$$\left(\lambda_p \frac{\partial q_p^2}{\partial n}\right)_{wall} = 0 \quad (4)$$

These boundary conditions are referred to as free-slip BC in this work.

In practical flow configurations, $\Sigma_{w,\tau n}$ takes positive value and increases with the particle-wall friction and wall roughness effect. However, according to Fede et al. (2016), the flux transferred by the particles towards the wall is limited by the transport effect within the particle assembly, accounted for by using the viscosity assumption, and such a maximum value is obtained for a zero particle tangential velocity condition at the wall. Therefore, the corresponding BC are

$$\left(U_{p,\tau}\right)_{wall} = 0 \quad (5)$$

$$\left(\lambda_p \frac{\partial q_p^2}{\partial n}\right)_{wall} = 0 \quad (6)$$

These BC are referred to as no-slip BC in this study.

Finally, as pointed out by Johnson and Jackson (1987), $\Sigma_{w,\tau n}$ may be written as the sum of a collisional and frictional contributions: $\Sigma_{w,\tau n} = \Sigma_{w,\tau n}^{col} + \Sigma_{w,\tau n}^{fr}$. The first contribution corresponds to the frictional effect due to the short particle contacts with the wall occurring when particles are in a wide space and bounce off the wall. The second contribution corresponds to the effect of particle contacts with the wall sustained for long times, which may occur when particles are very close to each other and slide together along the wall.

In the case of Coulomb's law for full sliding collisions on a flat surface with a friction coefficient μ_w^{col}, $\Sigma_{w,\tau n}^{col}$ may be written as (Sakiz and Simonin, 1999):

$$\Sigma_{w,\tau n}^{col} = \mu_w^{col} \left(\alpha_p \, \rho_p \frac{2}{3} \, q_p^2\right)_{wall} \quad (7)$$

$\Sigma_{w,\tau n}^{fr}$ may then be written as the product of a Coulomb friction coefficient, μ_w^{fr}, and the wall-normal component of the particle-wall frictional stresses, $\Sigma_{w,nn}^{col}$. In practice, $\Sigma_{w,nn}^{col}$ is assumed to be nearly identical to the inter-particle frictional pressure $P_p^{fr}(\alpha_p)$ given as an empirical function of the particle volume fraction $\alpha_p\big|_{wall}$ computed at particle center distance $d_p/2$ from the wall (Johnson and Jackson, 1987 ; Srivastava and Sundaresan, 2003). Finally, the particle-wall BC accounting for friction are written as

$$\left(\mu_p \frac{\partial U_{p,\tau}}{\partial n}\right)_{wall} = \mu_w^{col}\left(\alpha_p \rho_p \frac{2}{3} q_p^2\right)_{wall} + \mu_w^{fr} P_p^{fr}\left(\alpha_p|_{wall}\right) \quad (8)$$

$$\left(\lambda_p \frac{\partial q_p^2}{\partial n}\right)_{wall} = 0, \quad (9)$$

where the two Coulomb coefficients are depending on the particle and wall properties.

We may point out that the second term on the right-hand side of Eq. (8) is the dominant contribution in the dense regions of the system. In contrast, the frictional pressure is taken equal to zero for particle volume fraction less than $\alpha_{p,min} = 0.55$ and the only remaining contribution to particle friction at the wall is the collisional contribution which is proportional to the particle volume fraction α_p and to the random kinetic energy q_p^2.

Experimental system and simulation setup

The CLC system reproduced by the unsteady 3D numerical simulation is a 150 kW_{th} pilot operating at SINTEF Energy Research (Trondheim, Norway). A schematic diagram of the unit is given in Fig. 1. It is composed of two reactors, the air reactor (AR) and the fuel reactor (FR), each connected with its own cyclone and loop seal, and a lifter allowing the particles to flow from FR to AR according to the CLC design. AR dimensions are 23 cm in diameter and 6 m in height, and FR dimensions are 15.4 cm in diameter and 6.7 m in height (including lifter). In the experiments, the oxygen carrier is ilmenite from Titania A/S in Norway. Particle mean diameter (D_{50}) and bulk density are 90 μm and 2600 kg/m^3, respectively. In the numerical simulations, spherical particles with same mean properties are used, and a total mass inventory of 125.9 kg, estimated by the experiments, is imposed. Gas properties are computed at the temperature of 1273 K, which represents a mean temperature value of the CLC system at such operating point. Mass flow rates are chosen according to the experimental conditions, with the exception of the FR inlet, which is supplemented by the amount of volatiles released by the biomass during the pyrolysis, estimated by the proximate analysis. Mass flow rates are given in Table 1. Pressure boundary conditions at the two cyclone outlets are estimated from the experiments.

Table 1. Gas inlet flow rates

Item	Value (kg/h)	Item	Value (kg/h)
Primary gas of AR	146.67	AR loop seal, inlet leg	2.23
Secondary gas of AR, G1	17.04	AR loop seal, outlet leg	3.21
Secondary gas of AR, G2	29.16	FR loop seal, inlet leg	2.15
Inlet of FR	27.82	FR loop seal, outlet leg	1.73
Inlet of Lifter	2.27		

Table 2. Parameters for particle-wall boundary conditions

		μ_w^{col}	μ_w^{fr}
Case 1	No-slip BC	--	--
Case 2	Free slip BC	(0.0)	(0.0)
Case 3	Friction BC	0.5	0.5
Case 4	Friction BC	0.5	0.0

Numerical simulations are performed using NEPTUNE_CFD, which is a multiphase CFD code based on a cell-center type finite volume method and a first order temporal scheme (Neau et al., 2020). The CLC geometry is modeled by a mesh of about 0.76 million cells. Simulations are performed using 144 cores (4 nodes) corresponding to a mean computational cost of about 278 hours per second of physical time. A multiphase version of the k-ε model is used to predict the gas turbulence accounting for the effect of the particulate phase on the fluid flow. This model is coupled with an uncorrelated collision model for the particle random kinetic energy prediction. More details can be found in Hamidouche et al. (2019). In order to study the effects

of the particle-wall BC, different BC are used. Table 2 gives the corresponding parameters for each test case.

Results and discussion

Fig. 1 (first on the left) shows the distribution of the time-averaged relative pressure in the CLC system for Case 3, as an example. In the numerical simulation, pressure is taken at the center of the reactors (but it was found radially uniform inside). In the experiments, pressure was measured by transmitters (Fuji Electric, model FKCW33V5AKCYYAU, 0 – 320 mbar, 4 – 20 mA signal), mounted together on a skid / panel with 10 or 12 mm pipes to their respective pressure measurement points. They are differential pressure transmitters, but the reference pressure is to the atmosphere (the low-pressure entrance of the transmitter is open to the atmosphere) (Bischi et al. (2013)). The pressure is minimum at the top of the reactors and maximum at the bottom of the lifter, as expected. The pressure is much larger in the bottom part of the FR than in the bottom part of the AR, corresponding to a much larger solid inventory, about three times larger for Case 3 (using frictional BC as shown by Table 1). The distribution of the instantaneous solid volume fraction predicted by using frictional BC is shown by Fig. 1 (second on the left). The corresponding time animations show that in the AR, operating in a circulating regime, solids are transported by the fluidization gas to be separated by the cyclone. Then, these particles are sent to the FR through a loop seal. In the FR, solids are transported downward and injected in the AR through the Lifter, but some particles are also transported upward towards the cyclone, to be separated and reinjected in the AR through the loop seal. Results show that the solid volume fraction is higher in the FR than in the AR due to the different fluidization gas velocity, but the solid mass flow rate transported in FR to the cyclone represents only a small part of the total solid circulation rate (about 10%).

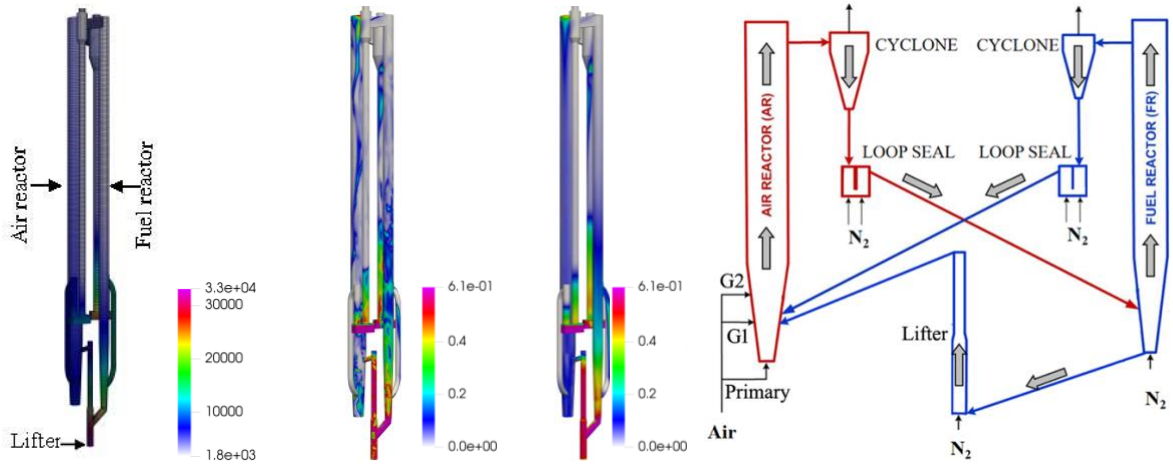

Fig. 1. From the left to the right: time-averaged relative pressure, instantaneous solid volume fraction, time-averaged solid volume fraction, for frictional wall BC (Case 3), schematic diagram of the CLC.

Fig. 2 shows the vertical profiles of time-averaged relative pressure predicted by using different BC. Results are globally in a good agreement with experimental data. However, significant differences in the mean pressure predictions may be observed between simulation results according to the wall BC used for the particle phase velocity. Fig. 2 (left) shows a comparison of the different boundary conditions in the AR. The figure shows a more rapid development of the linear pressure profile and less accumulation of solid in the bottom part of the reactor for no-slip than for free-slip BC. Fig. 2 shows that the pressure profiles obtained with partial friction BC corresponding to Case 4 (μ_w^{col} = 0.5, μ_w^{fr} = 0) are nearly identical to the free-slip BC predictions, meaning that the BC representing only the short-time frictional collision with a flat wall has a negligible effect on the flow behavior, as also shown in dense fluidized bed configuration by Fede et al. (2016). In contrast, Fig. 2 shows that the full friction BC (μ_w^{col} = 0.5, μ_w^{fr} = 0.5) has an effective effect on the mean pressure profiles but it is more difficult to analyze. As a matter of fact, according to the values of the solid volume fraction

predicted in the AR along the wall ($\alpha_p < 0.2$), the long-time friction BC contribution represented by μ_w^{fr} = 0.5 should not have any influence in this part of the system. Indeed, Fig. 2 (left) shows that the corresponding pressure profile in AR has a very similar shape than the pressure profile obtained in the free-slip case in terms of the height of the acceleration region and the extension of the linear pressure profile region, but the total mass and flow rate in the AR are smaller than in the free-slip case (see Fig. 4 and 5). So we may expect that the differences observed between the predictions of Case 3 (full friction) and those of Case 2 (free-slip) and Case 4 (partial friction) are mainly due to the effect of the long-time friction effect in the Lifter and in the FR, but also in the connecting pipes, which leads to modify the coupling conditions with the AR in the bottom region and to reduce the global circulation rate.

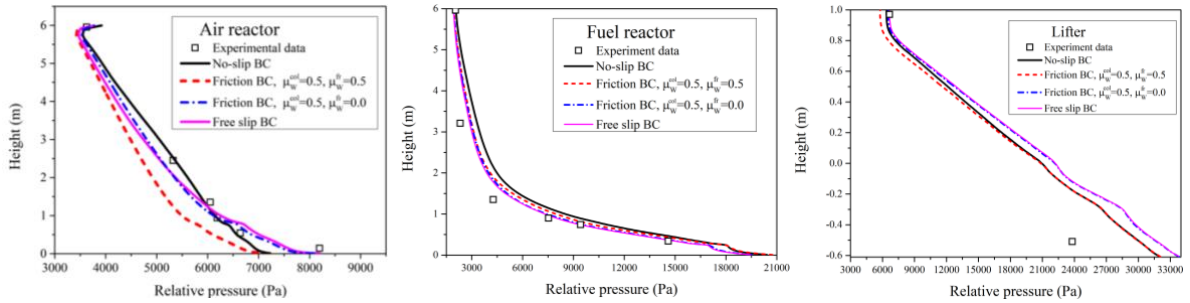

Fig. 2. Vertical profiles of time-averaged relative pressure. AR: left; FR: center; Lifter: right.

Radial profiles of time-averaged vertical solid velocity in AR and FR are displayed in Fig. 3 at a height far from connections. Particles flow up in the center and flow down near the wall. Negative velocities are detected in both the AR and FR in the region near the wall. As shown by the figure, in the AR, the time-averaged vertical velocities predicted using frictional BC are close to the one of simulation using free-slip BC, in the center. However, the asymmetry at the wall leads to conclude that these results are not statistically converged. In the FR, such differences are smaller.

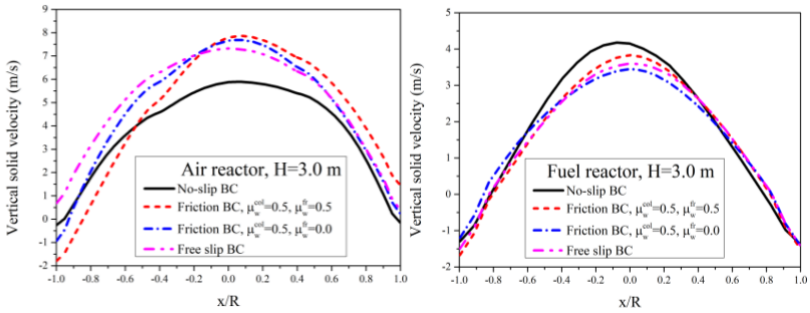

Fig. 3. Time-averaged vertical solid velocity. AR: left; FR: right.

The simulated flow rates of solids leaving the reactors from the top, based on different BC, are shown in Fig. 4. A substantial amount of solids leave the AR from the top, because it operates as a circulating fluidized bed. For the FR, most particles leave from bottom and enter the AR through the Lifter. The mass distributions in the different parts of the CLC, obtained using different BC, are shown in Fig. 5. The solid mass obtained in the FR based on free-slip and partial frictional BC (μ_w^{fr} = 0) are very similar. While, the mass based on a full frictional model (μ_w^{fr} = 0.5) is similar to that obtained with no-slip BC. In the Lifter and in the AR, the mass inventory is decreasing with the increase of the frictional effect, from free-slip to no-slip BC, and this effect is depending on the amount of solid inventory in the connecting parts of the system (cyclones, loop seals, pipes).

Conclusions

3D unsteady numerical simulations of a CLC system were carried out using the NEPTUNE_CFD multiphase code based on a two-fluid model approach. Several BC modeling assumptions were tested on a dual fluidized bed configuration corresponding to a pilot

operating at SINTEF, Trondheim, Norway. The predicted time-averaged vertical pressure profiles were analyzed and compared with the experimental measurements. Radial profiles of the time-averaged solid vertical velocity, as well as the solid mass distribution and flow rate were also shown for various BC models. The analysis pointed out the dominant particle-wall frictional effect of the long-time contacts in the Lifter and in the FR and the negligible particle-wall frictional effect of short-time collisions in the AR. The friction model is particularly suitable for prediction of systems with complex structures and different flow regimes. Further study should be carried out to analyze the effect of the wall roughness or irregular particle shape which may increase the particle-wall friction particularly in the dilute configuration of the AR.

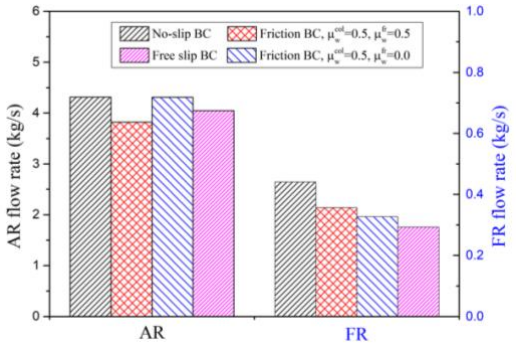

Fig. 4. Time-averaged solid mass flow rates at the top of the AR and FR.

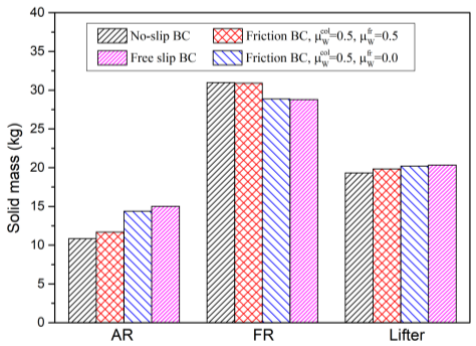

Fig. 5. Time-averaged distribution of solids in the different parts of the CLC.

References

Bischi, A., Langørgen, Ø., Bolland, O. Double loop circulating fluidized bed reactor system for two reaction processes, based on pneumatically controlled divided loop-seals and bottom extraction/lift. Powder Technol. 2013. 246, 51-62.

Fede, P., Simonin, O., Ingram, A. 3D numerical simulation of a lab-scale pressurized dense fluidized bed focussing on the effect of the particle-particle restitution coefficient and particle–wall boundary conditions. Chem. Eng. Sci. 2016. 142, 215-235.

Hamidouche, Z., Masi, E., Fede, P., Simonin, O., Mayer, K., Penthor, S. Unsteady three-dimensional theoretical model and numerical simulation of a 120-kW chemical looping combustion pilot plant. Chem. Eng. Sci. 2019. 193, 102-119.

Johnson, P. C., Jackson, R. Frictional-collisional constitutive relations for granular materials, with application to plane shearing. J. Fluid Mech. 1987. 176, 67–93.

Lyngfelt, A., Leckner, B., Mattisson, T. A fluidized-bed combustion process with inherent CO2 separation; application of chemical-looping combustion. Chem. Eng. Sci. 2001. 56, 3101–3113.

Neau, H., Pigou, M., Fede, P., Ansart, R., Baudry, C., Mérigoux, N., Laviéville, J., Fournier, Y., Renon, N., Simonin, O. Massively parallel numerical simulation using up to 36,000 CPU cores of an industrial-scale polydispersed reactive pressurized fluidized bed with a mesh of one billion cells. Powder Technol. 2020. 366, 906–924.

Sakiz, M., Simonin, O. Development and validation of continuum particle wall boundary conditions using Lagrangian simulation of a vertical gas/solid channel flow. Proc. 8th Int. Symp. on Gas-Particle Flows, ASME Fluids Engineering Division Summer Meeting. 1999.

Srivastava, A., Sundaresan, S. Analysis of a frictional-kinetic model for gas-particle flow. Powder Technol. 2003. 129, 72–85.